Biochimica et Biophysica Acta 1818 (2012) 219–224

Contents lists available at SciVerse ScienceDirect

Biochimica et Biophysica Acta

journal homepage: www.elsevier.com/locate/bbamem

A reinterpretation of neutron scattering experiments on a lipidated Ras peptide using replica exchange molecular dynamics ☆

Alexander Vogel [a], Matthew Roark [b], Scott E. Feller [b,*]

[a] Institute of Medical Physics and Biophysics, University of Leipzig, Härtelstr. 16-18, D-04275 Leipzig, Germany
[b] Department of Chemistry, Wabash College, 301 W. Wabash Ave. Crawfordsville IN 47933, USA

ARTICLE INFO

Article history:
Received 6 June 2011
Received in revised form 10 August 2011
Accepted 11 August 2011
Available online 18 August 2011

Keywords:
Molecular dynamics
Ras protein
Neutron scattering
Replica exchange

ABSTRACT

The Ras family of proteins plays crucial roles in a variety of cell signaling networks where they have the function of a molecular switch. Their particular medical relevance arises from mutations in these proteins that are implicated in ~30% of human cancers. The various Ras proteins exhibit a high degree of homology in their soluble domains but extremely high variability in the membrane anchoring regions that are crucial for protein function and are the focus of this study. We have employed replica exchange molecular dynamics computer simulations to study a doubly lipidated heptapeptide, corresponding to the C-terminus of the human N-Ras protein, incorporated into a dimyristoylphosphatidylcholine lipid bilayer. This same system has previously been investigated experimentally utilizing a number of techniques, including neutron scattering. Here we present results of well converged simulations that describe the subtle changes in scattering density in terms of the location of the peptide and its lipid modifications and in terms of changes in phospholipid density arising from the incorporation of the peptide into the membrane bilayer. The detailed picture that emerges from the combination of experimental and computational data exemplifies the power of combining isotopic substitution neutron scattering with atomistic molecular dynamics simulation. This article is part of a Special Issue entitled: Membrane protein structure and function.

1. Introduction

Ras proteins are GTP binding proteins that play a crucial role as molecular switches in signal transduction cascades responsible for cell growth, differentiation, and apoptosis. They are peripheral membrane proteins consisting of a soluble domain and a membrane anchor. Mutations in the soluble part of these proteins are known to inhibit their ability to become deactivated. In the past these mutations have been linked to the development of tumors and in fact in about 30% of all human tumors mutated forms of Ras proteins are found [1].The different human Ras variants are highly homologous exhibiting differences only in the C-terminal linker and membrane anchoring domains that contain varying numbers of lipid modifications. These lipid modifications (sometimes in conjunction with clusters of positively charged amino acids) are responsible for membrane association and their removal leads to inactive protein. While the structure of the soluble domain of a Ras protein was solved more than 20 years ago [2] little was known about the membrane anchoring domain at the time. In the last decade however considerable progress has been made in understanding topology, structure, and dynamics of the membrane anchors of human N-Ras, K-Ras, and H-Ras [3–12] using a large number of methods including neutron scattering, solid state nuclear magnetic resonance (NMR) spectroscopy, and increasingly molecular dynamics (MD) simulations.

The human N-Ras protein features a C-terminal membrane anchoring domain containing two post-translational palmitoyl lipid modifications. It is now commonly understood that the function of biological macromolecules not only depends on a single lowest energy conformer but rather to involve an ensemble of structures and the same has been found for the membrane anchor of human N-Ras. Recently we carried out a study that combined NMR spectroscopy with MD simulation to elucidate these structural fluctuations [4]. It was further shown that sufficient sampling of the peptide backbone structure could only be achieved by means of replica exchange MD simulations [13].

In the present study we have investigated the lipid–protein interactions that are key to N-Ras function by determining the location of the peptide backbone and the lipid modifications relative to the positions of a 1,2-dimyristoyl-sn-glycero-3-phosphocholine (DMPC) phospholipid bilayer membrane, a system for which there is extensive experimental structural data [3,12,14–19]. Our focus here is the use neutron scattering results [17] for the proteolipid complex to validate atomistic molecular dynamics computer simulations carried out on a system of molecules identical to the experimental conditions. While the experimental data is of fairly low resolution (best case: 6 orders of diffraction, nominal resolution of 8.5 Å, worst case: 3 orders of diffraction, nominal resolution of 19 Å), after showing that the simulations can quantitatively reproduce

☆ This article is part of a Special Issue entitled: Membrane protein structure and function.

* Corresponding author.
E-mail address: fellers@wabash.edu (S.E. Feller).

0005-2736/$ – see front matter © 2011 Elsevier B.V. All rights reserved.
doi:10.1016/j.bbamem.2011.08.016

the scattering results we can confidently use the extremely high resolution provided by the MD to obtain a detailed picture of the lipid–protein assembly. In the next section we described the computational approach taken to carry out and analyze the simulations, including the use of replica exchange molecular dynamics to enhance sampling. This is followed by comparison of simulation results with the neutron scattering data and the molecular level interpretation of this data that emerges from the analysis of simulation. We conclude with a discussion of potential future applications of this combined experimental–simulation approach to the challenging problem of structural characterization of membrane protein systems.

2. Methods

Both the experiments and simulations utilized a heptapeptide from the C-terminus of N-Ras with sequence gly-cys-met-gly-leu-pro-cys where both cysteines are covalently linked to hexadecyl chains which resemble the post translational palmitoylations in the full length protein but were chosen for improved stability in the experimental investigations. Two replica exchange MD simulations were conducted where one consisted of 40 DMPC lipids and 1119 waters while the other consisted of four Ras peptides, 40 DMPC lipids, and 984 waters in a periodically replicated cell. The system size, while atypically small for a membrane simulation, was chosen to optimize the exchange of conformations among the different temperatures in the replica exchange simulation. Setup of the initial conditions for both the lipid and peptides are described in reference [4]. The program CHARMM was employed for the simulation and its analysis [20], using the CHARMM all-H CMAP protein force field [21] with the all-H lipid force field [22]. The smooth particle-mesh Ewald algorithm [23] was used to compute the electrostatic forces and the SHAKE algorithm [24] was used to maintain rigid all bonds involving hydrogen atoms, allowing a 2-fs time step. All simulations were run under conditions of constant volume to remain system integrity at higher temperatures of the replica exchange. Both simulations were carefully monitored and membrane disintegration was not observed at any temperature.

The replica exchange technique was employed to enhance sampling of the backbone conformations which we previously showed are extraordinarily challenging to sample using conventional MD [4]. In total, 34 replicas were simulated at temperatures ranging from 303 K to 514 K. Spacing of the temperatures was adjusted such that the probability to accept a swap of replicas in neighboring temperatures (attempted every 250 fs) was ~10%. The replica exchange simulation of the pure DMPC membrane was run for 50.7 ns while the simulation with the N-Ras peptides present was run for 39.2 ns following an equilibration replica exchange simulation that was run for 54.2 ns. All data presented here were taken from the lowest temperature bath at 303 K (identical to the experimental conditions).

To calculate simulated neutron scattering profiles from MD, atoms that were deuterated in the experiments, were considered deuterated in the simulation. The simulation cell was divided into slices perpendicular to the z axis to create a histogram of atomic distributions along the membrane normal. Each bin was parallel to the plane of the bilayer with a width of 1.0 Å. Each trajectory frame was shifted such that the center of mass of the bilayer is centered at $z = 0$. In each trajectory frame the number of occurrences of atom a within bin b, n_{ab}, is multiplied by its corresponding scattering length, s_a [25]. The summation was accumulated for each bin over the entire trajectory. Next, the average for each bin was calculated by dividing by the total number of trajectory frames, the area of the simulation unit cell, and the number of bins. The result is a neutron scattering profile averaged over the entire MD simulation with an effective resolution of 1.0 Å. The same method was also used to compute profiles for particular atom groups simply by counting only the occurrences of atoms in that group.

3. Results and discussion

Fig. 1 provides a cartoon representation of the studied lipid/peptide/water system and summarizes the experimental findings published previously [17]. Several experiments were conducted to determine the location of the individual Ras groups by measurement of neutron scattering density difference profiles, i.e. the difference between the measured membrane profiles with and without peptide. The strategy that was employed is based on contrast variation between hydrogen and deuterium (deuterium scatters neutrons much more effectively) to localize differently labeled groups. For example, one profile was recorded for pure DMPC-d_{54} that was fully labeled with deuterium in the hydrocarbon region while another profile was recorded for the same lipid in presence of the Ras peptide without any deuterium atoms. The dilution of the highly scattering deuterium atoms in the DMPC molecules due to the presence of the peptide shows up in the difference of the two profiles (green line on the right hand side in Fig. 1) thereby revealing the location of the Ras lipid modifications. In a similar fashion the peptide backbone and the amino acid side chains were localized (red line on the right hand side in Fig. 1) and showed two distinct maxima. While it was tempting to speculate that the inner maximum corresponds to the side chains of the hydrophobic amino acids partitioning into the membrane hydrocarbon core and the outer maximum to the peptide backbone the low nominal resolution of the experiment never allowed such a detailed analysis. In summary these profiles were interpreted such that the peptide backbone is located in the lipid water interface and the lipid modifications as well as the hydrophobic side chains penetrate the hydrocarbon center of the host membrane but did not allow an exact localization.

Fig. 2 shows the scattering profiles from experiment and simulation, with and without the Ras peptide, as well as the difference profile, for each of the two deuteration schemes employed. Panel A shows the experimental neutron scattering density profiles of acyl chain deuterated lipid DMPC-d_{54} (red), DMPC-d_{54}/Ras (blue), and the difference between them (black). In this case the most prominent feature is expected to arise from the Ras lipid modifications because the protiated Ras lipid modifications, that mostly feature atoms with a small scattering cross section, dilute the strongly scattering deuterated DMPC acyl chains. In panel B the corresponding profiles calculated from the replica exchange simulations are presented. For the calculation of these profiles it was assumed that all ^{1}H atoms in the acyl chains of DMPC were replaced by ^{2}H thereby creating DMPC-d_{54}. Despite the large difference in resolution the agreement between simulation and experiment is excellent, both in terms of bilayer structural features, such as the hydrocarbon thickness and methyl trough width, and in the width and relative height of the difference profile. There is a small discrepancy in that the simulations do not reproduce the small outer

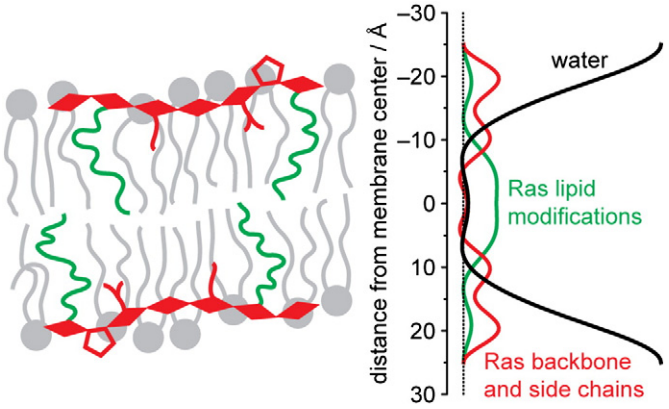

Fig. 1. Schematic representation of the structural model of the human N-Ras membrane anchor.
Reproduced from Ref. [17] with permission.

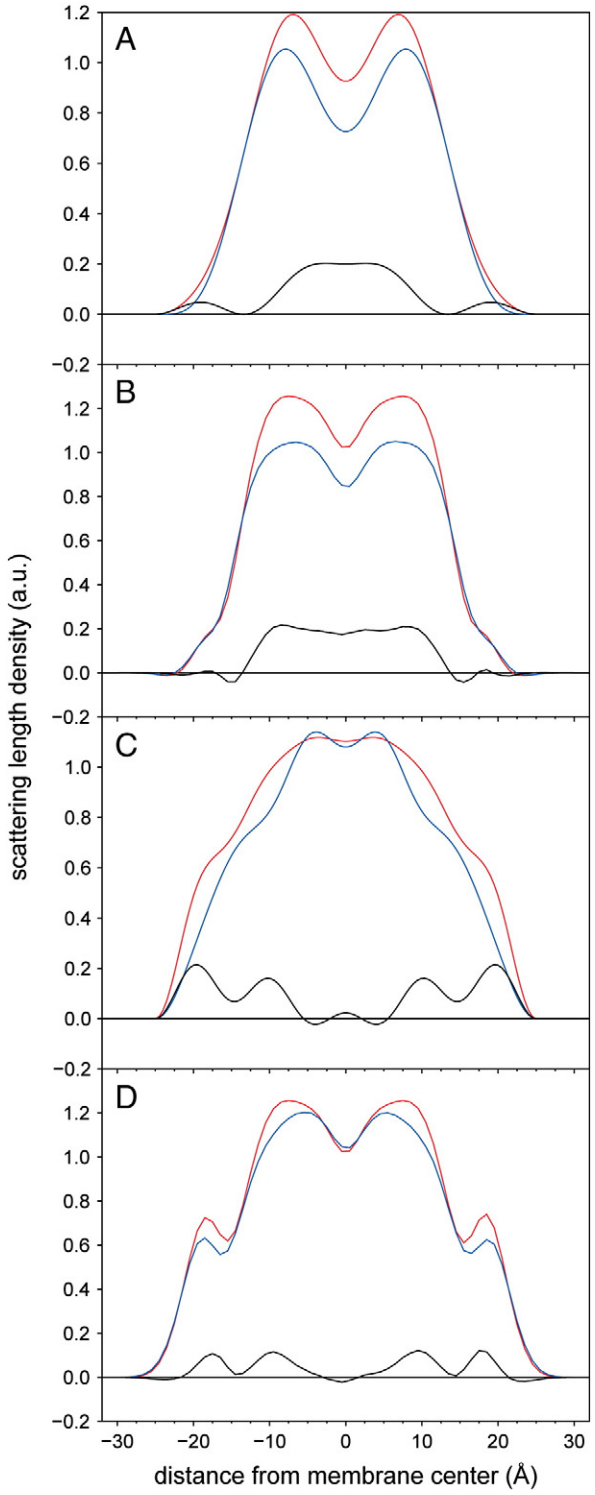

Fig. 2. Comparison of neutron scattering density profiles from experiment and simulation. Panel A shows the experimental neutron scattering density profiles of DMPC-d_{54} (red), DMPC-d_{54}/Ras (blue) and the difference between them (black) obtained from 3 orders of diffraction yielding a nominal resolution of 19 Å. Panel B shows the corresponding profiles calculated from the replica exchange simulations at a resolution of 1 Å. Profiles for a second deuteration strategy, DMPC-d_{67} (red) and DMPC-d_{67}/Ras-d_{66} (blue), were acquired from experiment (panel C, 6 orders of diffraction, nominal resolution 8.5 Å) and simulation (panel D, resolution: 1 Å) and the according difference profiles calculated (black). All data was gathered at 303 K.

peak in the difference profile at ~20 Å from the bilayer center, but this may well be an artifact of Fourier truncation since the hydrocarbon thickness of DMPC extends ~13 Å from the bilayer center [26], making it unlikely that significant change in mean scattering length densities is occurring this far from the deuterated acyl chains. The efficiency of sampling provided by the replica exchange technique is apparent when comparing the scattering profiles in the upper and lower monolayers of the bilayer. The agreement between the two halves of the bilayer shows that the statistical uncertainty in the simulation is extremely small, e.g. of the order of the line widths.

Panels C and D of Fig. 2 present data that parallel that of panels A and B but with a second deuteration scheme. In order to probe the location of the peptide backbone and amino acid side chains, experiments were carried out with deuterated Ras acyl chains, so that the difference profile in the hydrocarbon core will be minimized because deuterium concentrations will be approximately constant, and with phospholipids deuterated in both the acyl chains and the hydrophilic headgroups. Profiles of DMPC-d_{67} (red) and DMPC-d_{67}/Ras-d_{66} (blue) are shown from experiment (Fig. 2C) and simulation (Fig. 2D). The profiles show significantly more structure than those in panels A and B but again good agreement between simulation and experiment is observed in particular for the difference profile, e.g. the pair of peaks in the upper hydrocarbon and headgroup regions. Similarity between the scattering profiles from simulation and experiment could be further increased by smoothing the profiles from the simulations to correct for the much lower nominal resolution of the experiments but since the agreement is already very good for the difference profile which is most interesting to us without smoothing, we decided to keep the original data with higher resolution.

Having established that the simulation models can reproduce the experimental observables with good accuracy we now turn to analysis of the simulation trajectories. In Fig. 3 we present a decomposition of the difference profile from Fig. 2B, i.e. the DMPC chain deuterated case. From the replica exchange simulations neutron scattering density profiles were calculated for individual parts of the molecules. Scattering density originating from methyl (dashed) and methylene (solid) groups of the DMPC (red) and DMPC/Ras (blue) replica exchange simulations is shown. The differences between these two simulations were calculated for methyl and methylene groups and added up to give the solid green line which is virtually superimposed on the difference profile from Fig. 2B (solid black line). Thus we see clearly that the experimentally observed total scattering profile difference arises entirely from dilution of the DMPC hydrocarbon groups by the Ras peptide lipid modifications that are deeply embedded in the membrane as seen in the simulation snapshot shown in Fig. 4. The uniform dilution across the hydrophobic core is consistent with the observation, from simulation and ^{2}H NMR chain order

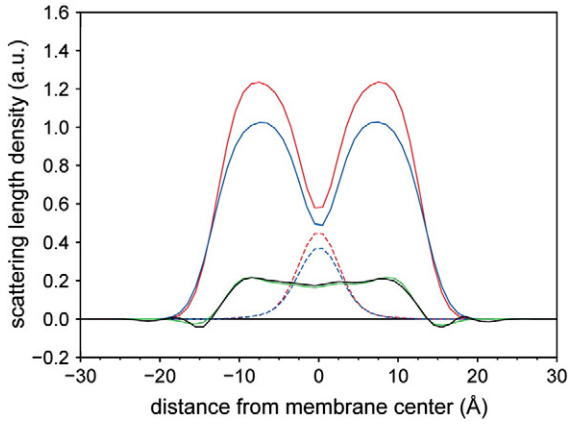

Fig. 3. Decomposition of the difference profile from Fig. 2B into contributions arising from methyl (dashed) and methylene (solid) groups of DMPC-d_{54} (red) and DMPC-d_{54}/Ras (blue). The differences between these two simulations were calculated for methyl and methylene groups and added up to give the solid green line which is virtually superimposed on the difference profile from Fig. 2B (solid black line).

parameters, that the Ras chain length adopts to the DMPC acyl chain length [5,18].

In Fig. 5 we analyze the difference profile from Fig. 2D (DMPC-d_{67}/Ras-d_{66}). It was originally hypothesized that the observed peaks in the difference profile arise from the protiated peptide backbone (outer peak) and the protiated hydrophobic side chains (inner peak) which dilute the ^{2}H atoms of the DMPC-d_{67} molecules but due to the low resolution of the experimental data, this could never be validated. This interpretation assumed that these features provided direct information on the location of the peptide in the bilayer [17]. The analysis of the simulation trajectories shows that the scattering density originating from the peptide backbone (blue), however, is actually located somewhere in between the two peaks, in direct contradiction to the original interpretation. The peptide backbone gives rise to no features in the difference profile due to an interesting cancelation of two effects. The reason why the dilution due to the backbone is not seen in the difference profile is the close match of the positive contribution of the backbone itself (shown in blue) and the negative contribution due to the dilution of the carbonyl groups whose difference profile between DMPC-d_{67} and DMPC-d_{67}/Ras-d_{66} simulations is shown in red. Their close lateral position can also be appreciated in the simulation snapshot shown in Fig. 7A.

While the analysis of the simulations shows that the peaks in the difference profile of DMPC-d_{67} and DMPC-d_{67}/Ras-d_{66} do not directly indicate the peptide location it does provide an interpretation of the observed peaks in terms of changes in lipid bilayer structure arising from peptide incorporation. We first examine the origin of the outer peak in the difference profile in terms of the DMPC phosphate and choline groups (Fig. 6A). In panel A the scattering density originating from choline (solid) and phosphate (dashed) groups of the DMPC-d_{67} (red) and DMPC-d_{67}/Ras-d_{66} (blue) replica exchange simulations is shown. The differences between these two simulations are shown as solid green and dashed green line respectively and are well superimposed with the outer peak in the difference profile from Fig. 2D (black). From the figure we see that the outer peak comes mainly from a dilution of the deuterated DMPC-d_{67} choline group that arises from greater spacing between lipid headgroups upon peptide incorporation which is also detailed in the simulation snapshot shown in Fig. 7B. In Fig. 6B we see that the origin of the inner peak in the

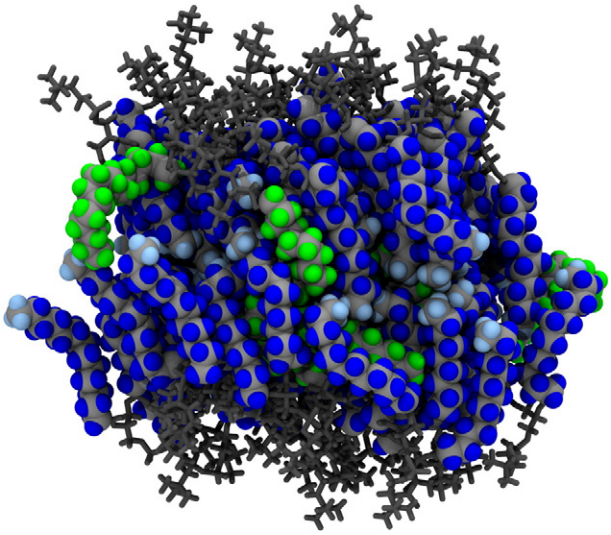

Fig. 4. Snapshot of the DMPC-d_{54}/Ras simulation detailing the observations from Fig. 3. All molecules except water are shown as gray sticks with the methyl and methylene groups of DMPC-d_{54} (hydrogens in cyan and blue respectively) and Ras (hydrogens in green) shown in a VdW representation.

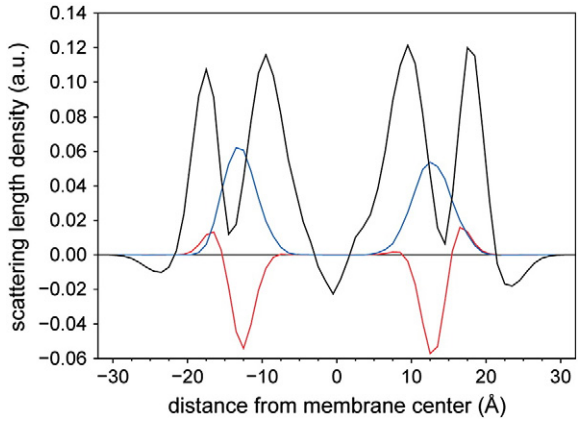

Fig. 5. Analysis of the difference profile from Fig. 2D (black) evaluating contributions arising from the Ras peptide backbone (blue) and the DMPC carbonyl groups (red) which virtually cancel each other.

difference profile arises from subtle changes in the structure of the hydrophobic core. The scattering density originating from methyl and methylene groups of the DMPC-d_{67} (red) and DMPC-d_{67}/Ras-d_{66} (blue) replica exchange simulations is shown and their difference (green) nicely overlaps with the inner peak in the difference profile from Fig. 2D (black). This small difference in hydrocarbon chain scattering corresponds to the location of the protonated hydrophobic side chains of the Ras peptide that dilute the deuterated

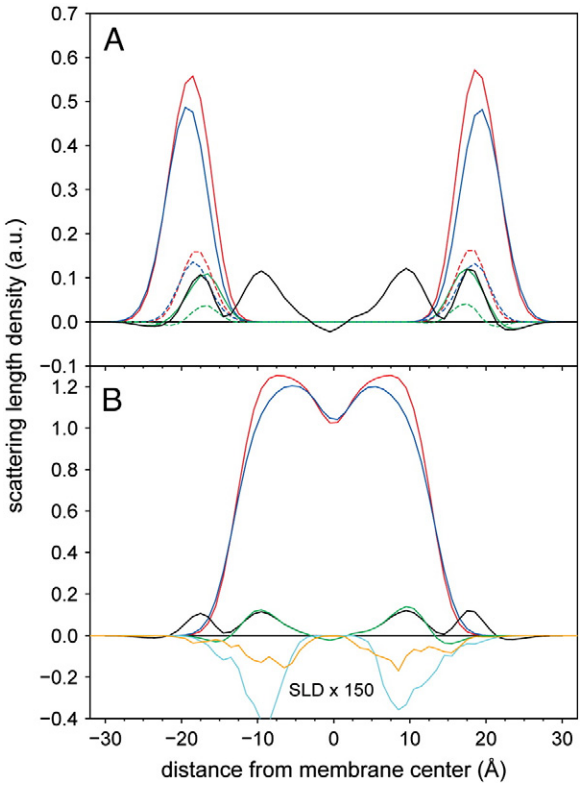

Fig. 6. Decomposition of the difference profile from Fig. 2D (black). Panel A shows scattering density originating from choline (solid) and phosphate (dashed) groups of the DMPC-d_{67} (red) and DMPC-d_{67}/Ras-d_{66} (blue) replica exchange simulations and the corresponding difference profiles (green). Panel B shows the scattering density originating from methyl and methylene groups of the DMPC-d_{67} (red) and DMPC-d_{67}/Ras-d_{66} (blue) replica exchange simulations and their corresponding difference profiles (green). Sidechain contributions from the peptide are shown as orange (methionine) and cyan (leucine) lines where their scattering profiles have been multiplied by 150.

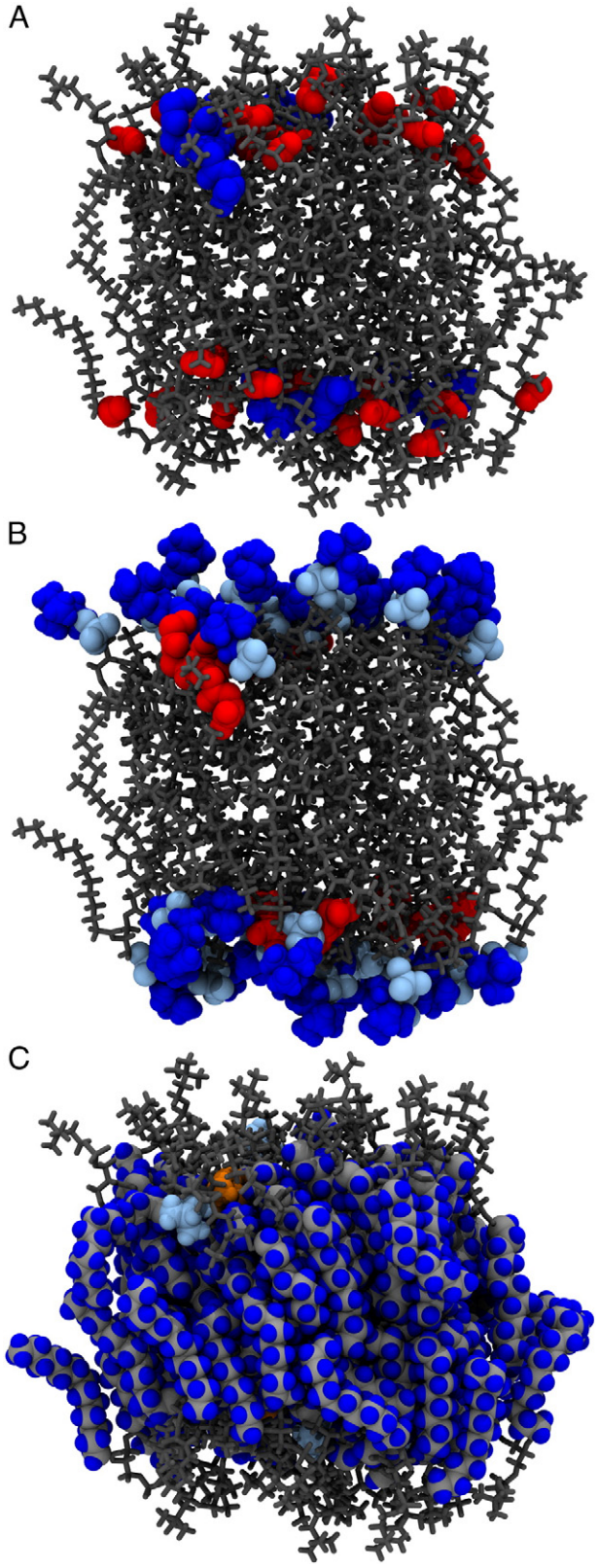

Fig. 7. Snapshots of the DMPC-d_{67}/Ras-d_{66} simulation detailing the observations from Figs. 5 and 6. All molecules except water are shown as gray sticks with highlighted moieties shown in a VdW representation. In panel A the Ras peptide backbone (blue) and the DMPC carbonyl groups (red) are shown which virtually are at the same lateral position. In Panel B the lipid choline (blue) and phosphate (cyan) groups that are diluted due to the presence of the Ras peptide backbone (red) in the lipid water interface are shown. Panel C shows the dilution of the methyl and methylene groups (hydrogens in blue) of DMPC-d_{67} and Ras-d_{66} close to the lipid water interface by the hydrophobic side chains of methionine (orange) and leucine (cyan).

groups (shown in expanded scale at the bottom of Fig. 6B). This can also be seen in the simulation snapshot shown in Fig. 7C.

4. Conclusions

Interpretation of neutron scattering profiles in particular when using molecules with isotopic labels often seems to be a fairly straightforward task once they have been calculated. Frequently, difference profiles are calculated to localize the labeled groups. Our results however show that one must be careful as the differences might not always arise solely from the addition of the labeled molecules but also by the influence they have on the system. In particular it was shown that one peak observed in such a difference profile purely originated from a change in system topology the peptide induced rather than from the peptide itself. In this case the circumstances were exceedingly unlucky since two different effects combined to make interpretation much more difficult. First, the peptide backbone that was to be located by the experiments was residing near the carbonyl groups, i.e. in the region of the membrane which cannot be deuterated. Therefore, the difference in scattering length was negligible as mostly carbon, oxygen and hydrogen of the lipids was replaced carbon, oxygen, hydrogen, and some nitrogen of the peptide backbone. Second, the peptide penetrated the membrane thereby pushing the lipids aside and diluting the deuterated headgroups generating a peak in the difference profile due to a secondary effect not allowing any direct conclusions about the peptide backbone location.

Our results show how atomistic computer simulations can be combined with low resolution neutron scattering data to obtain structural details of lipid–protein assemblies and avoid ambiguities in the interpretation. In such a combined approach the investigator can use the experiments solely to guide the simulations and validate their results while the simulations provide a detailed atomistic model of the physical system that allows a much more detailed interpretation. In the case investigated in this article we could now locate the peptide backbone of the membrane anchor of the human N-Ras protein with much more precision at the position of the lipid carbonyl groups. This position is about 4 Å closer to the membrane center than assumed before and much more precise than the experiment that offered a nominal resolution of either 8.5 Å or 19 Å. Regarding investigations on the structure and dynamics of the lipid modifications this offers new possibilities of data interpretation. Previously, it has been shown that the lipid modifications of Ras adopt their length to the surrounding membrane [5,18] and are therefore extremely flexible [19]. Lipid modifications of other proteins however do not react to changes in membrane thickness [6] and the underlying biophysical reasons are still not understood. Obviously, the position of the peptide backbone will be an important factor for the interactions as shown for in particular for MARCKS and Src where the backbone is located at the level of the head groups [27,28] which has dramatic effects on the acyl chain structure and dynamics [29]. Therefore, the much more precise position of the peptide backbone obtained in this article now provides the basis for new investigations on the molecular origin of these observations.

The simulation can also be used to reduce the number of neutron scattering experiments which must be carried out. For example, in the case of the Ras peptide/lipid bilayer system described here a possible experimental strategy would have been to prepare additional sets of samples that differed only in the deuteration schemes employed to Ras and the lipids. For instance samples could have been prepared with the composition DMPC-d_{54}/Ras where the Ras acyl chains were either protiated or deuterated. The difference profile in this case would have directly provided the location of the Ras acyl chains. Similarly, deuterating the peptide side chains and measuring the difference profile against a membrane containing Ras with protiated side chains would identify the location of these groups. It is

unclear, however, if the significant efforts and expense to conduct these additional experiments would be worth the additional information gleaned. In the former case, i.e. comparing Ras acyl chains, there is no additional insight provided over the experiments and simulations described here. And in the latter case of very costly amino acid deuteration one would still be left without information on the location of the backbone.

In summary, we could show that MD simulations are well suited to complement neutron scattering experiments. They greatly simplify interpretation of the experimental results and provide much more information than could be deducted from the experiments alone.

Acknowledgements

We thank the National Science Foundation for support under award MCB-0950258. We thank Richard Venable for providing the scripts for implementing REXMD using CHARMM.

References

[1] A. Wittinghofer, H. Waldmann, Ras — a molecular switch involved in tumor formation, Angew. Chem. Int. Ed. 39 (2000) 4193–4214.
[2] E.F. Pai, W. Kabsch, U. Krengel, K.C. Holmes, J. John, A. Wittinghofer, Structure of the guanine–nucleotide-binding domain of the Ha-Ras oncogene product P21 in the triphosphate conformation, Nature 341 (1989) 209–214.
[3] G. Reuther, K.T. Tan, A. Vogel, C. Nowak, K. Arnold, J. Kuhlmann, H. Waldmann, D. Huster, The lipidated membrane anchor of full length N-Ras protein shows an extensive dynamics as revealed by solid-state NMR spectroscopy, J. Am. Chem. Soc. 128 (2006) 13840–13846.
[4] A. Vogel, G. Reuther, M.B. Roark, K.T. Tan, H. Waldmann, S.E. Feller, D. Huster, Backbone conformational flexibility of the lipid modified membrane anchor of the human N-Ras protein investigated by solid-state NMR and molecular dynamics simulation, Biochim. Biophys. Acta Biomembranes 1798 (2010) 275–285.
[5] A. Vogel, G. Reuther, K. Weise, G. Triola, J. Nikolaus, K.T. Tan, C. Nowak, A. Herrmann, H. Waldmann, R. Winter, D. Huster, The lipid modifications of Ras that sense membrane environments and induce local enrichment, Angew. Chem. Int. Ed. 48 (2009) 8784–8787.
[6] A. Vogel, T. Schroder, C. Lange, D. Huster, Characterization of the myristoyl lipid modification of membrane-bound GCAP-2 by H-2 solid-state NMR spectroscopy, Biochim. Biophys. Acta Biomembranes 1768 (2007) 3171–3181.
[7] D. Abankwa, A.A. Gorfe, K. Inder, J.F. Hancock, Ras membrane orientation and nanodomain localization generate isoform diversity, Proc. Natl Acad. Sci. USA 107 (2008) 1130–1135.
[8] D. Abankwa, A.A. Gorfe, J.F. Hancock, Mechanisms of Ras membrane organization and signaling: Ras on a rocker, Cell Cycle 7 (2008) 2667–2673.
[9] A.A. Gorfe, M. Hanzal-Bayer, D. Abankwa, J.F. Hancock, J.A. McCammon, Structure and dynamics of the full-length lipid-modified H-ras protein in a 1,2-dimyristoylglycero-3-phosphocholine bilayer, J. Med. Chem. 50 (2007) 674–684.
[10] L. Janosi, A.A. Gorfe, Segregation of negatively charged phospholipids by the polycationic and farnesylated membrane anchor of Kras, Biophys. J. 99 (2010) 3666–3674.
[11] S. Lukman, B.J. Grant, A.A. Gorfe, G.H. Grant, J.A. McCammon, The distinct conformational dynamics of K-Ras and H-Ras A59G, Plos Comput. Biol. 6 (9) (2010) e1000922.
[12] G. Reuther, K.T. Tan, J. Kohler, C. Nowak, A. Pampel, K. Arnold, J. Kuhlmann, H. Waldmann, D. Huster, Structural model of the membrane-bound C terminus of lipid-modified human N-ras protein, Angew. Chem. Int. Ed. 45 (2006) 5387–5390.
[13] Y. Sugita, Y. Okamoto, Replica-exchange molecular dynamics method for protein folding, Chem. Phys. Lett. 314 (1999) 141–151.
[14] F. Bringezu, M. Majerowicz, S.Y. Wen, G. Reuther, K.T. Tan, J. Kuhlmann, H. Waldmann, D. Huster, Membrane binding of a lipidated N-Ras protein studied in lipid monolayers, Eur. Biophys. J. Biophys. Lett. 36 (2007) 491–498.
[15] D. Huster, Investigations of the structure and dynamics of membrane-associated peptides by magic angle spinning NMR, Prog. Nucl. Magn. Reson. Spectrosc. 46 (2005) 79–107.
[16] D. Huster, K. Kuhn, D. Kadereit, H. Waldmann, K. Arnold, H-1 high-resolution magic angle spinning NMR spectroscopy for the investigation of a Ras lipopeptide in a lipid membrane, Angew. Chem. Int. Ed. 40 (2001) 1056-+.
[17] D. Huster, A. Vogel, C. Katzka, H.A. Scheidt, H. Binder, S. Dante, T. Gutberlet, O. Zschornig, H. Waldmann, K. Arnold, Membrane insertion of a lipidated Ras peptide studied by FTIR, solid-state NMR, and neutron diffraction spectroscopy, J. Am. Chem. Soc. 125 (2003) 4070–4079.
[18] A. Vogel, C.P. Katzka, H. Waldmann, K. Arnold, M.F. Brown, D. Huster, Lipid modifications of a Ras peptide exhibit altered packing and mobility versus host membrane as detected by 2H solid-state NMR, J. Am. Chem. Soc. 127 (2005) 12263–12272.
[19] A. Vogel, K.-T. Tan, H. Waldmann, S.E. Feller, M.F. Brown, D. Huster, Flexibility of Ras lipid modifications studied by 2H solid-state NMR and molecular dynamics simulations, Biophys. J. 93 (2007) 2697–2712.
[20] B.R. Brooks, R.E. Bruccoler, B.D. Olafson, D.J. States, S. Swaminathan, M. Karplus, CHARMM: a program for macromolecular energy, minimization, and dynamics calculations, J. Comput. Chem. 4 (1983) 187–217.
[21] A.D. MacKerell, M. Feig, C.L. Brooks, Improved treatment of the protein backbone in empirical force fields, J. Am. Chem. Soc. 126 (2004) 698–699.
[22] J.B. Klauda, B.R. Brooks, A.D. MacKerell Jr., R.M. Venable, R.W. Pastor, An ab initio study on the torsional surface of alkanes and its effect on molecular simulations of alkanes and a DPPC bilayer, J. Phys. Chem. B 109 (2005) 5300–5311.
[23] U. Essmann, L. Perera, M.L. Berkowitz, T. Darden, H. Lee, L.G. Pedersen, A smooth particle mesh Ewald method, J. Chem. Phys. 103 (1995) 8577.
[24] J.P. Ryckaert, G. Ciccotti, H.J.C. Berendsen, Numerical integration of the cartesian equations of motion of a system with constraints: molecular dynamics of n-alkanes, J. Comput. Phys. 23 (1977) 327–341.
[25] M.C. Wiener, S.H. White, Structure of a fluid dioleoylphosphatidylcholine bilayer determined by joint refinement of X-ray and neutron diffraction data. III. Complete structure, Biophys. J. 61 (1992) 434.
[26] N. Kucerka, Y. Liu, N. Chu, H.I. Petrache, S. Tristram-Nagle, J.F. Nagle, Structure of fully hydrated fluid phase DMPC and DLPC lipid bilayers using X-ray scattering from oriented multilamellar arrays and from unilamellar vesicles, Biophys. J. 88 (2005) 2626–2637.
[27] A. Arbuzova, L.B. Wang, J.Y. Wang, G. Hangyas-Mihalyne, D. Murray, B. Honig, S. McLaughlin, Membrane binding of peptides containing both basic and aromatic residues. Experimental studies with peptides corresponding to the scaffolding region of caveolin and the effector region of MARCKS, Biochemistry 39 (2000) 10330–10339.
[28] D. Murray, L.H. Matsumoto, C.A. Buser, J. Tsang, C.T. Sigal, N. Ben-Tal, B. Honig, M.D. Resh, S. McLaughlin, Electrostatics and the membrane association of Src: theory and experiment, Biochemistry 37 (1998) 2145–2159.
[29] H.A. Scheidt, D. Huster, Structure and dynamics of the myristoyl lipid modification of Src peptides determined by H-2 solid-state NMR spectroscopy, Biophys. J. 96 (2009) 3663–3672.